Proceedings of the 1996 IEEE
International Conference on Robotics and Automation
Minneapolis, Minnesota - April 1996

Impact Dynamics of Space Long Reach Manipulators

Kazuya Yoshida*, Constantinos Mavroidis** and Steven Dubowsky**

* Dept. of Aeronautics and Space Engineering
Tohoku University, Aoba, Sendai 980-77, Japan
** Dept. of Mechanical Engineering
Massachusetts Institute of Technology
Cambridge, MA 02139, U.S.A.

Abstract

The problem of impact dynamics of space robotic systems that consist of a rigid manipulator supported by a flexible deployable structure is addressed. Due to joint backdrivability and the dynamic coupling between the manipulator and its supporting structure, unknown motion of the system occurs after it makes impulsive contact with the environment. A method that uses the system's dynamic model is proposed to estimate the motion of the system after impact. This method which can be used to find ways to minimize the impact effect and vibrations of the supporting structure due to impact, is verified experimentally using the MIT Vehicle Emulation System (VES II). The experimental results show that the impact force and the system motion after impact can be reduced if the manipulator configuration prior to impact and the controller gains are properly selected.

1. Introduction

Robotic systems supported by flexible long-reach deployable structures have been proposed for future space projects. The Special Purpose Dexterous Manipulator (SPDM) mounted on the Space Station Remote Manipulator System (SSRMS) (see Figure 1) and the Japanese Experiment Module Remote Manipulator System (JEMRMS) proposed by the Japan's NASDA, are examples of space long-reach manipulators now being developed [1], [2].

While promising, the development of long reach space manipulator systems requires the solution of fundamental technical problems. A key problem is the dynamic coupling between the manipulator and its flexible supporting structure. This causes uncontrolled motion of the manipulator supporting structure when the manipulator performs a task. This undesired base motion can degrade the system's performance, including its dexterity. The problem of vibrations of long reach manipulator systems when these

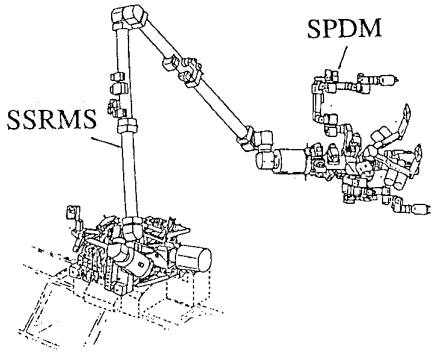

Figure 1 An example of a space long-reach manipulator: The Canadian SPDM and SSRMS [1]

are excited by the system's internal inertial forces has been studied [3], [4]. However, little has been done when the vibrations of the supporting structure are excited by external disturbances such as impact forces that act on the system when it makes contact with the environment. This problem can be critical when a long reach manipulator catches a passive free-floating object, such as a satellite. In this operation, substantial impact forces to the manipulator system can excite vibration of the flexible supporting structure.

The mechanical behavior of manipulators under impact is not well understood when the joints show *some* backdrivability even if they are ground-fixed. In ideal conditions, when the joints are either free-to-move or break-locked, the dynamics are well defined. However in real situations, due to friction, stiffness, damping, and inertia of the actuator and gear train, unknown manipulator joint motion is produced after impact. In addition, when the manipulator supporting structure is flexible, dynamic inter-

0-7803-2988-4/96 $4.00 © 1996 IEEE

action between the manipulator and its base will produce unknown vibratory motion of the system after impact.

A method called Extended-Inversed Inertia Tensor (Ex-IIT) has been proposed to obtain estimations of the impact forces and of the resulting system motion after impact [5]. These estimations can be extended in the system design phase to check its structural safety under impact, and in the planning phase to select optimal manipulator configurations to catch a free floating object so that impact forces are reduced. The Ex-IIT method can be applied in the case of manipulator systems with fixed, free-floating or flexible supporting structures and with joints that can be free, break-locked or back-drivable. The Ex-IIT method has been validated with simulations and verified experimentally using a planar two degree of freedom model of a free-floating manipulator system [5].

In this paper the problem of impact dynamics of long reach manipulator systems is studied experimentally in conditions that are close to reality. The Ex-IIT method is experimentally verified, using the MIT Vehicle Emulation System mod II (VES-II) testbed [6]. This system can emulate in real time, the spatial six degree of freedom (three translations and three rotations) of any free floating or flexibly supported manipulator system, in ground or microgravity conditions [7]. It consists of a 6 DOF hydraulically driven Stewart platform, a six degree of freedom force/torque sensor and any manipulator that can be mounted on the platform. For the experiments performed during this work a PUMA 560 was mounted on the platform. Impact conditions were produced at the tip of the manipulator end effector using a specially designed impact device. Experiments were performed using various controller gains and manipulator configurations. In a first phase the manipulator supporting structure was kept fixed. Then, in a second phase the VES emulated the motion of a flexible supporting structure for the manipulator. The motion of the manipulator system and that of its base after impact was recorded and compared to the estimation given by the Ex-IIT method. The experimental results verified Ex-IIT and showed that the manipulator configuration and the joint controller gains affect the magnitude of the impact force and the motion of the flexible supporting structure.

2. Modeling of Impact Dynamics

Collision of rigid bodies is a classical problem in mechanics ([8]). This phenomenon becomes very complex when the collided systems are subject to multibody or free-floating dynamics, or to friction and compliance effects. For ground based manipulator systems the problem of reducing the impact force has been addressed in [9]-[13]. Recently a method has been proposed to model impact dynamics of manipulator systems with friction and compliance characteristics at their joints supported by free-floating or ground-fixed bases, using an Extended-Inversed Inertia Tensor (Ex-IIT) [5]. The same method is used in this paper to study impact dynamics of manipulators supported by flexible strcutures.

In the Ex-IIT method, the effect of resistance impulse at joints is modeled as a Virtual Rotor Inertia at corresponding joints. Yoshikawa and Yamada [14] provided a mathematical proof by frequency domain analysis that a Virtual Rotor Inertia can represent joint stiffness and damping in the impulsive impact phase. In this paper, this idea is confirmed by experiments.

Let $\mathcal{F} = (\mathbf{f}^T, \mathbf{N}^T)^T \in R^6$ be an impact force/moment at the end-effector of a fixed base manipulator system, $\boldsymbol{\tau}_p \in R^n$ be a passive joint torque due to friction, compliance, and damping, and $\boldsymbol{\tau}_a \in R^n$ be an active joint torque due to servo control. The manipulator system dynamic equation takes the form:

$$\mathbf{H}\ddot{\boldsymbol{\phi}} + \mathbf{c}(\boldsymbol{\phi}, \dot{\boldsymbol{\phi}}) + \boldsymbol{\tau}_p + \boldsymbol{\tau}_a = \mathbf{J}^T\mathcal{F}, \tag{1}$$

where $\mathbf{H} \in R^{n\times n}$ is the system's inertia matrix, $\mathbf{c} \in R^n$ is a non-linear velocity dependent term, $\boldsymbol{\phi} \in R^n$ is the manipulator joint angle vector, $\mathbf{J} \in R^{6\times n}$ is the manipulator Jacobian matrix and n is the number of joint degrees of freedom of the manipulator.

Consider the integral of equation (1) for the impact period from t to $t+\delta t$ for a very small impact time period $\delta t \to \epsilon$:

$$\lim_{\delta t\to\epsilon}\int_t^{t+\delta t}(\mathbf{H}\ddot{\boldsymbol{\phi}} + \mathbf{c}(\boldsymbol{\phi}, \dot{\boldsymbol{\phi}}) + \boldsymbol{\tau}_p + \boldsymbol{\tau}_a)\mathrm{dt} = \lim_{\delta t\to\epsilon}\int_t^{t+\delta t}\mathbf{J}^T\mathcal{F}\mathrm{dt} \tag{2}$$

Usually the effect of terms such as $\mathbf{c}(\boldsymbol{\phi}, \dot{\boldsymbol{\phi}})$, $\boldsymbol{\tau}_p$, $\boldsymbol{\tau}_a$, is neglected because their integral during the infinitesimal impact period has a finite value. The terms $[\int_t^{t+\delta t}\mathbf{H}\ddot{\boldsymbol{\phi}}\mathrm{dt}]$ and $[\int_t^{t+\delta t}\mathbf{J}^T\mathcal{F}\mathrm{dt}]$ can take an infinite value and dominate the impact dynamics. However, for practical systems with non-negligible friction and other motion resistance at joint, it turns out that the joint torque effect $[\int_t^{t+\delta t}(\boldsymbol{\tau}_p + \boldsymbol{\tau}_a)\mathrm{dt}]$ is not neglected and, in this paper, accounted an effective element of the impact dynamics. Using the notation $(\ddot{\circ}) \to (\Delta\dot{\circ})$ to replace an instantaneous acceleration by the corresponding velocity change before and after the impact, equation (2) takes the form:

$$\mathbf{H}\Delta\dot{\boldsymbol{\phi}} + \mathbf{T} = \mathbf{J}^T\overline{\mathcal{F}} \tag{3}$$

where $\overline{\mathcal{F}} \in R^6$ represents impulse. Equation (2) will be called the "manipulator impact dynamics equation in joint space."

$\mathbf{T} \in R^n$ represents the joint effect of impulsive resistance against the external impact force, called the "joint

resistance impulse." This resistance impulse is due to friction, stiffness, damping and actuators under servo-control, and can relate to impulsive velocity change $\Delta\dot{\phi}$ before and after impact in the following way:

$$\mathbf{T} = \boldsymbol{\lambda}\Delta\dot{\phi}, \tag{4}$$

Then, equation (3) is written as:

$$(\mathbf{H} + \boldsymbol{\lambda})\Delta\dot{\phi} = \mathbf{J}^T\overline{\mathcal{F}} \tag{5}$$

The matrix coefficient $\boldsymbol{\lambda} \in R^{n\times n}$ is called Virtual Rotor Inertia and is considered to be an additional joint inertia, or an increased gear-ratio connected to the rotor of a joint actuator.

The impact dynamics equation in operational space can be written with respect to the manipulator end-effector in the following form:

$$\mathbf{G}^{*-1}\Delta\dot{\mathbf{x}}_h = \overline{\mathcal{F}} \tag{6}$$

where $\Delta\dot{\mathbf{x}}_h \in R^6$ is the difference of the end-effector velocities before and after the impact, and $\mathbf{G}^* \in R^{6\times 6}$ is called the Extended-Inversed Inertia Tensor. It is defined as:

$$\mathbf{G}^* \equiv \mathbf{J}(\mathbf{H} + \boldsymbol{\lambda})^{-1}\mathbf{J}^T \tag{7}$$

for ground-fixed manipulators.

For flexibly supported manipulator systems, such as the long reach systems that are studied here, $\mathbf{G}^*$ takes a similar form as in free-floating systems:

$$\mathbf{G}^* \equiv \mathbf{J}^*(\mathbf{H}^* + \boldsymbol{\lambda})^{-1}\mathbf{J}^{*T} + \mathbf{R}_{gh}\mathbf{M}^{-1}\mathbf{R}_{gh}^T \tag{8}$$

where $\mathbf{J}^* \in R^{6\times n}$ and $\mathbf{H}^* \in R^{n\times n}$ are the augmented forms of the system's Jacobian matrix and inertia matrix respectively [15]. The matrices $\mathbf{M}$ and $\mathbf{R}_{gh}$ are equal to: $\mathbf{M} = \begin{bmatrix} w\mathbf{E} & \mathbf{0} \\ \mathbf{0} & \mathbf{H}_g \end{bmatrix} \in R^{6\times 6}$ and $\mathbf{R}_{gh} = \begin{bmatrix} \mathbf{E} & -\tilde{\mathbf{r}}_{gh} \\ \mathbf{0} & \mathbf{E} \end{bmatrix} \in R^{6\times 6}$ where w and $\mathbf{H}_g$ are the total mass and inertia of the manipulator and its moving base with respect to the centroid, respectively, $\mathbf{r}_{gh}$ is a moment arm from the system centroid to the end-effector, and $\mathbf{E}$ is the 3×3 identity matrix. For detailed derivation of $\mathbf{G}^*$, see [5].

Consider the case where the manipulator end-effector collides with a moving object of mass m_b and velocity $\mathbf{v}_b \in R^3$. The manipulator end-effector velocity is $\mathbf{v}_a \in R^3$. At the moment of collision an impact force $\mathbf{f}$ is exerted at the manipulator end-effector at the contact point in a certain direction $\mathbf{n}$. It is assumed that no moment is developed at the manipulator end-effector during the impact. Using the principle of linear momentum conservation, equation (6) is written in the form:

$$\mathbf{G}_{33}^{*-1}\Delta\mathbf{v}_a = \overline{\mathbf{f}} = -m_b\Delta\mathbf{v}_b \tag{9}$$

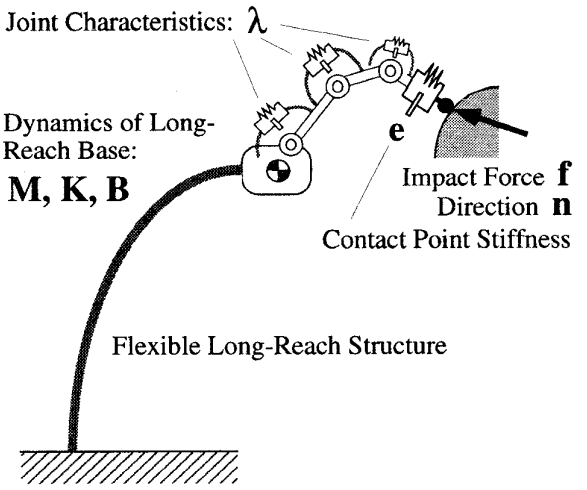

Figure 2 Dynamic model of space long reach manipulators

where $\mathbf{G}_{33}^*$ is the top-left 3×3 quadrant of the Ex-IIT associated with the linear motion.

If equation (9) is multiplied (inner product) with $\mathbf{n}$, the following scalar formula is obtained:

$$m_a^*(v_a' - v_a) = m_b(v_b - v_b') \tag{10}$$

where v_a and v_b are the projections of $\mathbf{v}_a$ and $\mathbf{v}_b$ on $\mathbf{n}$, $\{'\}$ indicates the velocity after collision, and

$$m_a^* \equiv \frac{|\mathbf{f}|}{|\dot{\mathbf{v}}_a|} = \frac{1}{\mathbf{n}^T\mathbf{G}_{33}^*\mathbf{n}} \tag{11}$$

is called the manipulator "effective mass" that expresses the inertial characteristics of the manipulator end-effector in the direction of the impact [16][17].

The "elastic restitution coefficient" e of the end-effector is defined by:

$$v_a' - v_b' = e(v_b - v_a). \tag{12}$$

From equations (10) and (12), the post-impact manipulator end-effector velocity and the magnitude of impulse can be obtained using pre-impact information:

$$v_a' = \frac{(1+e)m_bv_b + (m_a^* - em_b)v_a}{m_a^* + m_b} \tag{13}$$

$$\overline{\mathbf{f}} \cdot \mathbf{n} = \frac{(1+e)m_a^*m_b(v_b - v_a)}{m_a^* + m_b} \tag{14}$$

Note that in equations (13) and (14) the Virtual Rotor Inertia $\boldsymbol{\lambda}$ and the elastic restitution coefficient e are assumed to be known. These coefficients characterize the system

dynamics and can be found experimentally. The experimental procedure to identify these parameters is shown in sections 3 and 4.

The dynamic model of space long reach manipulators under impact is summarized as follows, using Figure 2. The contact point stiffness between the manipulator end-effector and environment is characterized by the restitution coefficient e. The instantaneous joint effect, including servo stiffening, against the impact force is characterized by the Virtual Rotor Inertia $\boldsymbol{\lambda}$. The values of e and $\boldsymbol{\lambda}$ will be identified by preliminary tests in ground-based condition, before launch in actual cases. The inertial characteristics of the base are incorporated in equation (8) using the system's mass matrix $\mathbf{M}$. In addition, the vibrational characteristics of the flexible long-reach structure are expressed by a stiffness matrix $\mathbf{K}$ and a damping matrix $\mathbf{B}$, which are usually obtained from a FEM model of the structure.

3. Experiment Methodology

The Extended-Inversed Inertia Tensor (Ex-IIT) method is experimentally verified using the MIT Vehicle Emulation System mod II (VES-II) [6]. This system consists of a 6 DOF hydraulically driven Stewart platform, a force/ torque sensor and a PUMA 560 mounted on the top of the platform (see Figure 3). When the manipulator moves or when it makes a contact with the environment, the resulting interaction forces and moments between the manipulator and its supporting structure are measured with the force/torque sensor. These forces and moments are used in a computer dynamic model of the flexible supporting structure of a long reach system and its motion is calculated under the measured load. Then the platform is commanded to reproduce this spatial six degree of freedom motion in real time. The VES can also be used to emulate the motion of these systems in micro-gravity conditions [7].

An impact device has been built to study impulsive contacts between the system and its environment (see Figure 3). The device is a pendulum with a steel hammer head. It is equipped with a piezo-electric sensor to measure the impact force and an encoder to be able to calculate the velocity of the impact head before and after impact.

In our experiments, the impact device hits the tip of the manipulator end-effector which is wrapped in a soft material. Results are presented for experiments with the manipulator base fixed and the VES emulating the motion of a flexible long-reach system. In each case, three manipulator configurations and three sets of joint control gains are tested. The three configurations are chosen to be representative of the manipulator workspace (see Figure 4). For example in configuration 2 the arm is relatively stretched while in configuration 3 it is relatively folded. The three sets of gains for the joint PID controller are characterized as High, Low and Zero and they represent situations where

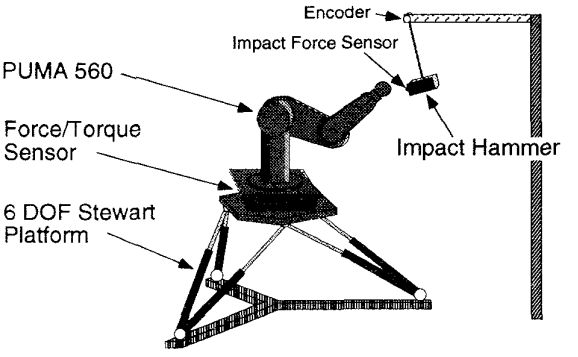

Figure 3 The MIT VES-II and the impact device

the arm is stiff, compliant or free to move. The specific parameters that describe the configurations and the sets of control gains are shown in Table 1.

For each configuration and set of gains, impacts with various impact velocities in the range of 1.0-2.5 [m/s] are applied. The values of the impact force exerted at the manipulator end-effector vary between 30-70 [N]. Only the first three joints of the manipulator are active. The impact force direction is kept parallel to the -x direction of the inertial reference system. In the case of Zero and Low gains, a constant torque is applied to the manipulator joints to compensate for gravity to assist the arm in holding its nominal position.

During the experiments, the manipulator system moves due to the impact. The joint angles of manipulator arm, the angle of the impact device, the base/manipulator interaction forces and moments, the impact force, the emulated moving base passive motion are all measured variables. The velocities of the end-effector and of the impact device before and after impact $v_a, v_b, v_a^{'}, v_b^{'}$ are calculated after the experiment by numerical differentiation. From equations (10) and (12) the manipulator effective mass and the restitution coefficient are calculated.

The purpose of these experiments is:

a) To calculate experimentally the manipulator effective mass and restitution coefficient and observe the way they depend on the manipulator configuration and controller gains.

b) To confirm the idea derived by the Ex-IIT method that the joint friction and controller gains increase the manipulator effective mass.

c) To show that the manipulator joint motion and the motion of its flexible supporting structure when there is an impact with the environment depend on the manipulator configuration prior to impact and the controller gains.

Table 1 Parameters of the experimental conditions

Configuration	joint 1	2	3
1	0 [deg]	150	90
2	0	172	40
3	0	135	135

Servo-gain	P	D	I
Zero	0	0	0
Low	5000	40	0
High	500000	4000	1500

(counts in a custom PID controller)

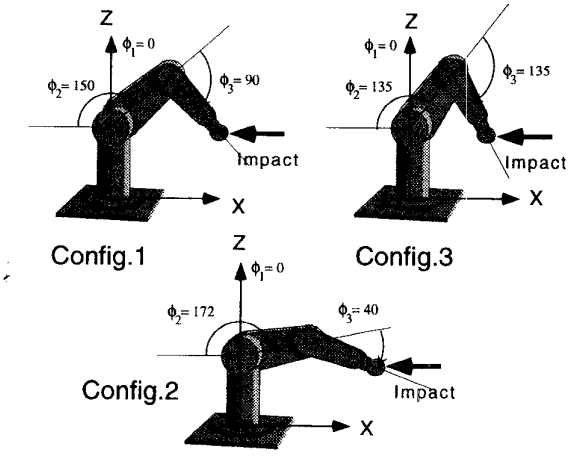

Figure 4 Arm configurations and impact direction

4. Experimental Results

4.1. Fixed-Base Experiments

The first experiments had the manipulator base fixed. The manipulator joint motion after impact is observed and the manipulator effective mass and restitution coefficient are calculated in each experiment.

In Figure 5 the motion of joint 3 after impact is shown as it was recorded during one of the experiments. In this experiment the manipulator prior to impact is at configuration 1, with zero gains. Due to impact the joint almost instantly moves about 2.5 degrees with a high velocity that is very quickly damped out. The sampling interval of this joint angle measurement is 20 [ms].

Using equations (10) and (12), the effective mass and the restitution coefficient are calculated for all the experiments performed and their values are shown in Figures 6 and 7, for zero (Z), low (L), and high (H) controller gains.

In Figure 6, the results show that the effective mass depends on both, the configuration and controller gains. In Configuration 3 (folded configuration) the effective mass is lower. In Configuration 1 which is characterized as

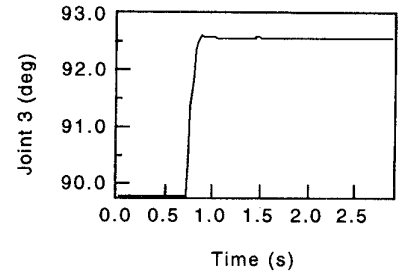

(a) joint displacement

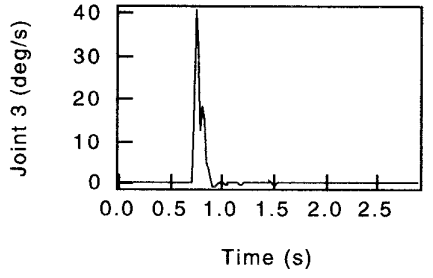

(b) joint velocity

Figure 5 Joint 3 motion after impact in Configuration 1 with Zero gains

intermediate, the effective mass increases. The effective mass obtains its higher value in Configuration 2 (stretched configuration). In the cases of Zero and Low gains the effective mass takes similar values which are much lower than in the case of High gains. This result supports the concept of Virtual Rotor Inertia that the joint torque effect increases the system virtual mass. The results also show that the impact effect can be reduced by properly selecting the manipulator configuration (eg folded configurations) and by using lower controller gains.

In Figure 7 the result show that the restitution coefficient is not a function of the manipulator configuration or the controller gains. It depends on the elasticity of the material of the contact point. For our experimental system it has an average value of 0.55. The variation of the values of the restitution coefficient as it is shown in Figure 7, during the experiments, is due to a small variation of the impact point and of the surface condition.

In Table 2 a comparison of the effective mass of an idealized model for the system used in these experiments and the experimentally measured effective mass, is presented. In the first column, the values of the effective mass are displayed as these are calculated using the Ex-IIT method with $\boldsymbol{\lambda} = \mathbf{0}$ that represents an idealized situation of the system with no joint resistance and no controller. The next two columns show experimental results of the system with joint

Table 2 Identified effective mass versus joint condition
(for fixed-base experiments)

Config.	Effective mass in [kg]			Ratio	
	Simulation	**Experiments**			
	Link Dynamics (m_1) (free joint)	Zero and Low gains (m_2) (+ joint friction)	High gain (m_3) (+ servo torque)	m_2/m_1	m_3/m_1
1	6.99	12.98	28.45	1.86	4.07
2	19.66	38.14	76.45	1.94	3.89
3	4.96	8.91	19.11	1.80	3.86

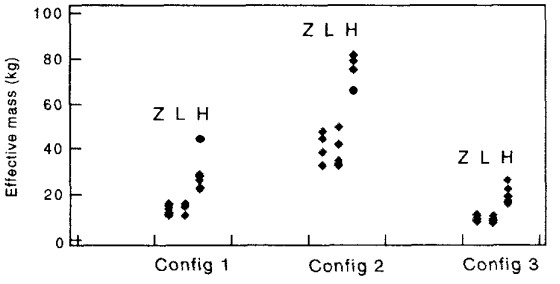

Figure 6 Observed effective mass
(Z=zero, L=low, H=high)

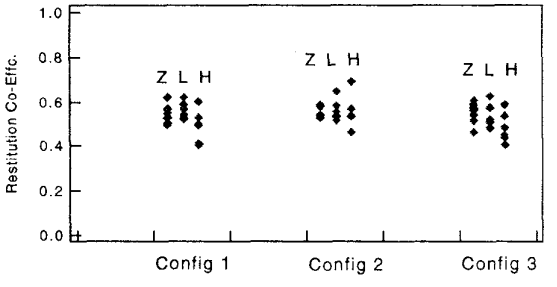

Figure 7 Observed restitution coefficient
(Z=zero, L=low, H=high)

resistance, including friction, stiffness, and damping torque (all represented with the term *friction* in Table 2), with or without control feedback. In the last two columns the ratio of the experimentally calculated values of the effective mass to the model based estimated values are shown. A general statement can be made that for the system used in these experiments, the existence of friction in the manipulator joints doubles the impact effect. The same statement can be made in the case of high gain joint PID control. These two results taken together, show that the impact effect becomes four times higher if friction and high gain control are present on the same time.

Knowing the effective mass that was calculated experimentally, the Virtual Rotor Inertia $\boldsymbol{\lambda}$ can also be calculated. Suppose that $\boldsymbol{\lambda}$ is a diagonal matrix. In that case, for the system used in these experimens $\boldsymbol{\lambda}$ has the form:

$$\boldsymbol{\lambda} = \text{diag}[\lambda_1, \lambda_2, \lambda_3] \tag{15}$$

Equation (11) is a function of the manipulator configuration including three unknowns: $\lambda_1, \lambda_2, \lambda_3$. If we have a set of equation (11) for three different configurations, we can obtain a closed-form system. The solution of this system gives $\lambda_1, \lambda_2, \lambda_3$. If $\boldsymbol{\lambda}$ is a full matrix more configurations should be taken into account in order to form a closed-form system. For our experimental system the values of $\lambda_1, \lambda_2, \lambda_3$ are listed in **Table 3**. Obviously these values depend on the controller gains.

4.2. Flexible Base Experiments

Experiments were performed with the VES-II system emulating the motion in microgravity conditions of a vertical flexible cylindrical beam with ($EI = 2.5 \times 10^8$[Pa · kgm^2]) that is assumed to be the supporting structure of the PUMA 560 (see Figure 8).

Figure 9 shows the displacement of the manipulator base from the initial position. Results are shown for configurations 1 and 2, for High gains and Low gains. Note that the motion is not a simple sinusoidal wave because the contact point is off-centered from the plane of symmetry of the three dimensional beam.

The experimental results show that the motion of the system supporting structure after impact is smaller if configuration 1 and/or Low control gains are used. On the other, the motion is much bigger if configuration 2 and/or High gains are used. The experimental data show a reduction of 20-30% of the maximum amplitude of base vibrations after impact when Low gains are used compared to High gain motion. These results indicate that there are configurations and gains that can reduce the system motion after impact.

Table 4 shows a comparison between the manipulator effective mass calculated in simulations using equation (8) and $\boldsymbol{\lambda}$ estimated by the fixed-base experiments, and the effective mass calculated experimentally using equation (10). These values show a good agreement and confirm the Ex-IIT method when it is applied in long reach manipulator systems.

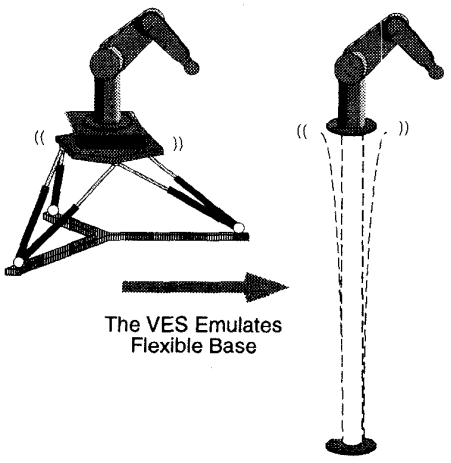

Figure 8 Flexible-base experiments

Table 3 Experimentally identified λvalues

	Virtual Rotor Inertia [kgm^2]	
	Zero and Low gains (friction dominant)	**High gain** (+ servo torque)
λ_1	19.82	53.18
λ_2	4.62	8.66
λ_3	0.80	2.83

Finally, an important observation is that the motion of the flexible based manipulator is smaller when the effective mass is small. This means that the effective mass can be used as an index to reduce vibrations of the supporting flexible beam.

5. Conclusions

Impact experiments with manipulators supported by fixed or flexible supporting structures have been performed using the MIT Vehicle Emulation System (VES-II). The experimental data revealed the following conclusions:

a) Fixed-base experiments:

- The restitution coefficient is not a function of the manipulator configuration or its joint control gains. It is related to the stiffness of the contact point.
- The effective mass at the manipulator end-effector depends on the manipulator configuration and joint control gains. Joint friction and servo torque increase the effective mass and therefore the impact effect. The experimental data support the Ex-IIT method.

b) Flexible base experiments:

- The amplitude of the supporting structure vibrations when these are excited by impulsive contacts of the system to the environment depends on the manipulator configuration and its control gains.
- The manipulator effective mass can be used as an index to reduce the motion of the supporting structure that results from impact.

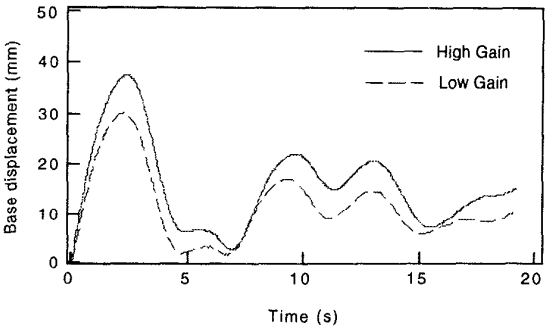

(a) Configuration 1

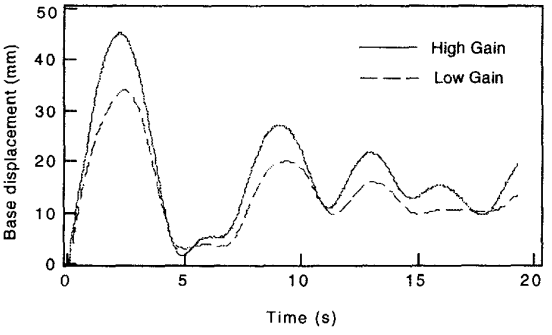

(b) Configuration 2

Figure 9 Manipulator base motion after impact

Table 4 Effective mass for flexible-base manipulator

Config	Gain	Effective mass in [kg]	
		Simulation using estimated λ	Experiment
1	Low	13.90	14.21
	High	21.89	20.98
2	Low	28.96	27.48
	High	38.99	39.33

The fact that lower PD gains can reduce the supporting structure vibrations induced by impact contacts of the long reach system with its environment suggests a close relevance to the Pseudo-Passive Energy Dissipation concept proposed by Torres [18] for vibrations of long reach systems when these are excited by the system's internal inertial forces and moments. In addition an optimal direction

of the impulsive manipulator motion in terms of minimum excitation of the supporting structure could be discussed with the Coupling-Map method [18], [19].

Acknowledgments

The support of this work by NASA Robotics Branch, Grant NAG 1-801 is acknowledged.

References

[1] Brimley, W., Brown, D. and Cox, B., "Overview of International Robot Design for Space Station Freedom," *Teleoperation and Robotics in Space, ed. by Skaar and Ruoff*, pp.411-441, Progress in Astronautics and Aeronautics vol.161, AIAA, 1994.

[2] Kuraoka, K. et al., "Design and Development Status of the JEMRMS," *Proc. of Int. Symp. on AI, Robotics and Automation in Space (i-SAIRAS'90)*, pp.23-26, Kobe, Japan, November, 1990.

[3] Dubowsky, S., "Dealing With Vibrations in the Deployment Structures of Space Robotic Systems," *5th International Conference on Adaptive Structures*, Sendai, Japan, December, 1994.

[4] Mavroidis, C., Rowe, P. and Dubowsky, S., "Inferred Endpoint Control of Long Reach Manipulator Systems," *Proc. of IEEE/RSJ Int. Symp. on Intelligent Robot System (IROS'95)*, Vol. 2, pp.71-76, Pittsburg, PA, August, 1995.

[5] Yoshida, K., "Impact Dynamics Representation and Control with Extended-Inversed Inertia Tensor for Space Manipulators," *Robotics Research 6, ed. by Kanade and Paul*, pp.453-463, IFRR, Cambridge, 1994.

[6] Dubowsky, S. et al., "A Labratory Test Bed for Space Robotics: The VES II," *Proc. of IEEE/RSJ Int. Symp. on Intelligent Robot System (IROS'94)*, Munich, Germany, pp.1562-1569, 1994.

[7] Corrigan, T. and Dubowsky, S., "Emulating Microgravity in Laboratory Studies of Space Robotics," *Proc. of the 23rd ASME Mechanisms Conference*, MN, USA, 1994.

[8] Wittenburg, J., *Dynamics of Systems of Rigid Bodies*, Stuttgart: B.G.Teubner, 1977.

[9] Zheng, Y.F. and Hemami, H., "Mathematical Modeling of a Robot Collision With its Environment," *Journal of Robotic Systems*, Vol.2, No.3, pp.289-307, 1985.

[10] Youcef-Toumi, K. and Gutz, D.A., "Impact and Force Control," *Proc. 1989 IEEE Conf. on Robotics and Automation*, Scottsdale, AZ, pp.410-416, May 1989.

[11] Gertz, M.W., Kim, J-O. and Khosla, P.K. "Exploiting redundancy to reduce impact force," *Proc. 1991 IEEE/RSJ Int. Workshop on Intelligent Robots and Systems (IROS'91)*, Osaka, Japan, pp.179-184, Nov. 1991.

[12] Walker, I.D., "Impact Configurations and Measures for Kinematically Redundant and Multiple Robot Systems," *IEEE Trans. on Robotics and Automation*, vol.10, no.5, pp.670-683, 1994.

[13] Lin, Z., Patel, R. and Balafoutis, C., "Impact reduction for Redundant Manipulators Using Augmented Impedance Control," *Journal of Robotic Systems* Vol. 12, No. 5, pp.301-313, 1995.

[14] S. Yoshikawa and K. Yamada, "Impact estimation of a space robot at capturing a target"' in *Proc. of 1994 IEEE/RSJ Int. Conf. on Intelligent Robots and Systems (IROS'94)*, pp. 1570–1577, Munich, 1994.

[15] *Space Robotics: Dynamics and Cotrol*, ed. by Xu and Kanade, Kluwer Academic Publishers, 1993.

[16] Khatib, O. and Burdick, J., "Motion and Force Control of Robot Manipulators," *Proc. 1986 IEEE Int. Conf. on Robotics and Automation*, San Francisco, CA, pp.1381-1386, April 1986.

[17] Asada, H. and Ogawa, K., "On the Dynamic Analysis of a Manipulator and Its End Effector Interacting with the Environment," *Proc. 1987 IEEE Int. Conf. on Robotics and Automation*, Raleigh, NC, pp.751-756, March-April 1987.

[18] Torres, M., *Modeling, Path-Planning and Control of Space Manipulators: The Coupling Map Concept*, PhD Thesis, Department of Mechanical Engineering, MIT, February 1993.

[19] Torres, M., Dubowsky, S. and Pisoni, A.C., "Path-Planning for Elastically-Mounted Space Manipulators: Experimental Evaluation of the Coupling Map," *Proc. 1994 IEEE Int. Conf. on Robotics and Automation*, San Diego, CA, pp.2227-2233, May 1994.